Supplementary Information for

Synergy of CuO and g-C_3N_4 for boosting hydrogen peroxide photosynthesis

Yuqing Pang,†[a] Yan Tian,†[a] Peng Zheng,[a] Ke Feng,[a] Jie Mao,[b] Yujun Zhu,[c] Kai Huang,[d] Fei Ke,*[a] and Chunyan Zhang*[a]

[a]Department of Applied Chemistry, School of Materials and Chemistry and State Key Laboratory of Tea Plant Biology and Utilization, Anhui Agricultural University, Hefei 230036, P. R. China.

E-mail: kefei@ahau.edu.cn (F. Ke); zhangchunyan@ahau.edu.cn (C. Zhang)

[b]School of Environment and Energy Engineering, Anhui Jianzhu University, Hefei 230022, P. R. China.

[c]Department of Pharmacy and Biomedical Engineering, Clinical College of Anhui Medical University, 1166 Wangjiang West Road, Hefei 230031, P. R. China.

[d]*Department of Chemistry and Molecular engineering, East China University of Science and Technology, Shanghai, 200237, P.R.China.*

†These authors contributed equally to this work.

Characterizations

Scanning electron microscopy (SEM) and transmission electron microscopy (TEM) are used to characterise and analyse the microstructural features of the samples. X-ray diffraction (XRD) is used to analyse the diffraction patterns of the materials to determine the crystalline structure of the materials, and X-ray electron spectroscopy (XPS) is used to measure the elemental composition of the various compounds. Moreover, the UV–vis spectra of the different materials were measured by UV–vis spectrometer. Besides, their electrochemical impedance spectra (EIS) and photocurrent responses were measured by the electrochemical work station, in which a three-electrode system was utilized consisting of the working electrode, a saturated calomel electrode (SCE) as the reference, and a platinum wire electrode as the counter one. Furthermore, the Mott-Schottky (M−S) plotting was performed to evaluate the flat band potentials of the photocatalytic materials, on the basis of the data of electrochemical measurements operated at an amplitude of 5.0 mV and a frequency of 1.0 kHz.

The concentration of H_2O_2 was determined by iodometric method, and the reaction equation was: $H_2O_2 + 3I^- + 2H^+ \rightarrow I_3^- + 2H_2O$, I^- in the solution was oxidized to I_3^- by H_2O_2, and then the absorbance of I_3^- was determined by UV spectrophotometry. The specific method was as follows: a series of H_2O_2 solutions with concentrations of 100 μmol/L^{-1}, 50 μmol/L^{-1}, 25 μmol/L^{-1}, 10 μmol/L^{-1}, 5 μmol/L^{-1} and 2.5 μmol/L^{-1}were prepared first. 1 mL of the above clear solution was taken respectively and added to complex a certain volume of fluorescent reagent (1 mL 0.4 mol/L^{-1} KI, 1 mL 0.1 mol/$L^{-1}$$KHC_8H_4O_4$) with the reaction system, and the reaction was carried out in the dark for 45 min for complete color development. At the same time, the reference solution was prepared with deionized water, and then the absorbance at λ=320-400 nm was detected with a UV spectrophotometer to obtain a maximum wavelength of 352 nm, the data were recorded, and a standard curve was made to calculate the concentration of H_2O_2.

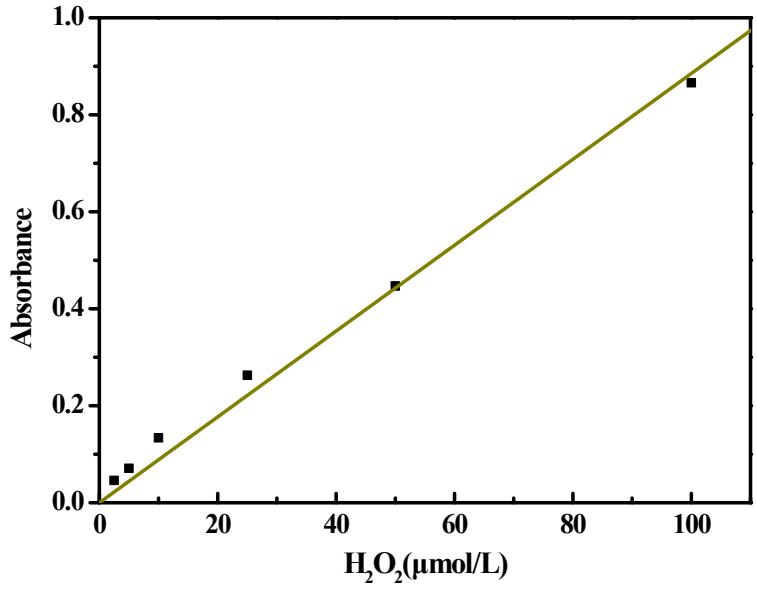

Fig. S1 Standard curve of H_2O_2 concentration

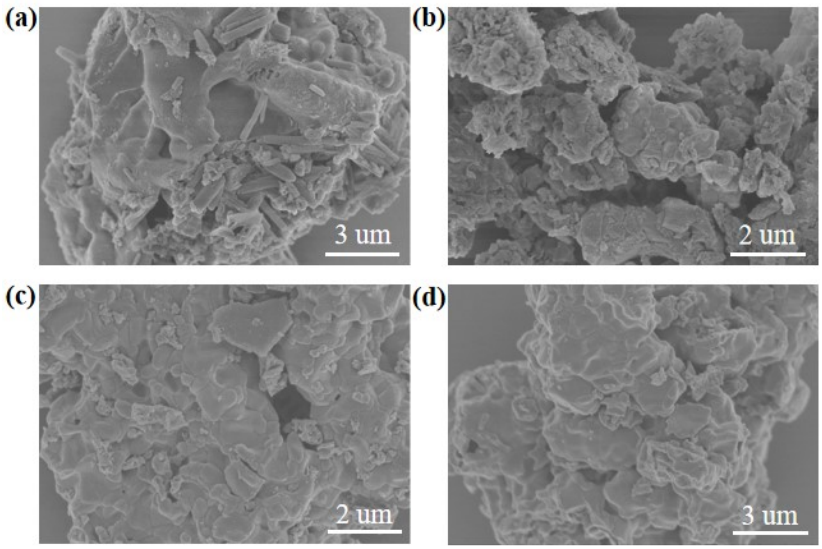

Fig. S2 SEM images of 10%-CuO/g-C_3N_4 (a), 20%-CuO/g-C_3N_4 (b), 40%-CuO/g-C_3N_4 (c), 50%-CuO/g-C_3N_4 (d).

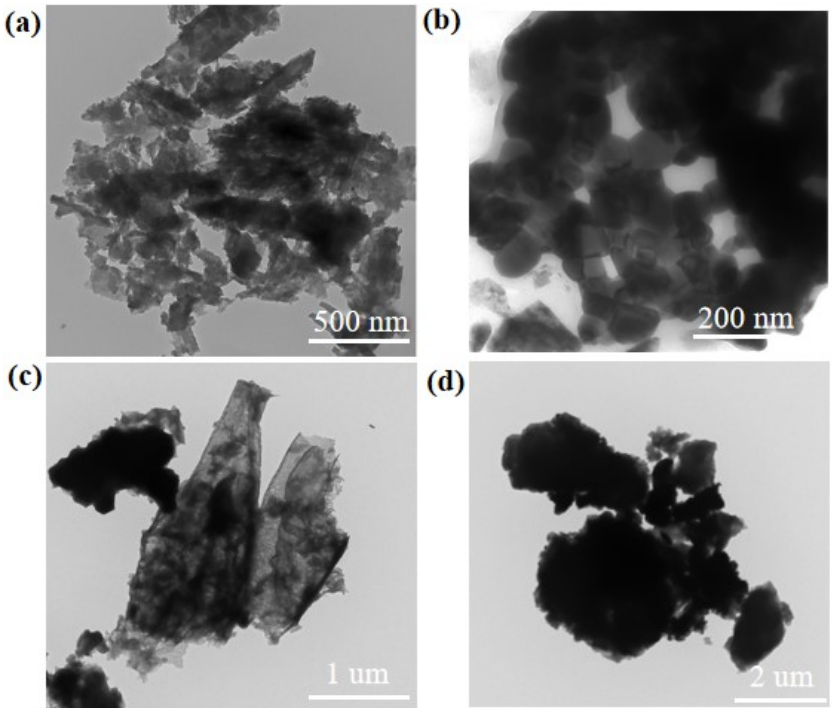

Fig. S3 TEM images of 10%-CuO/g-C_3N_4 (a), 20%-CuO/g-C_3N_4 (b), 40%-CuO/g-C_3N_4 (c), 50%-CuO/g-C_3N_4 (d).

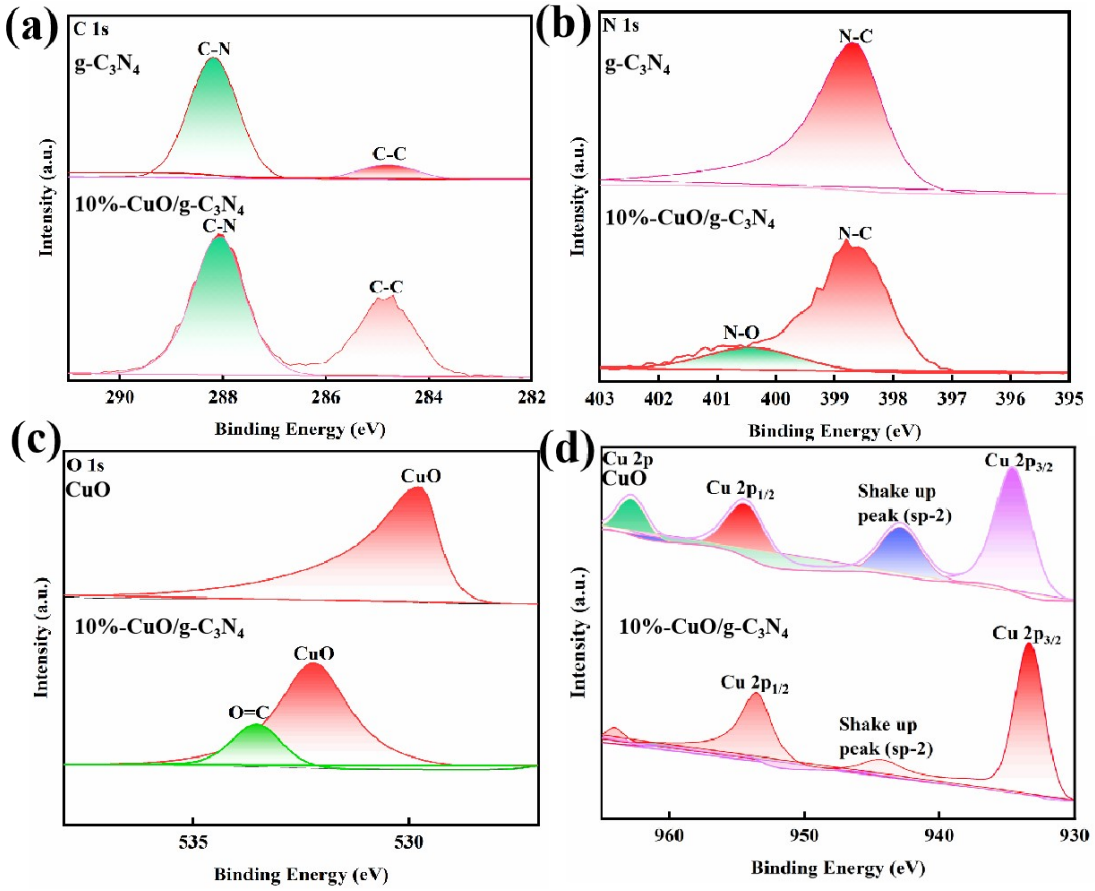

Fig. S4 The corresponding high-resolution XPS spectra of C 1s (a) N 1s (b), O 1s (c) and Cu 2p (d) of 10%-CuO/g-C_3N_4 in comparision with pure CuO and g-C_3N_4.

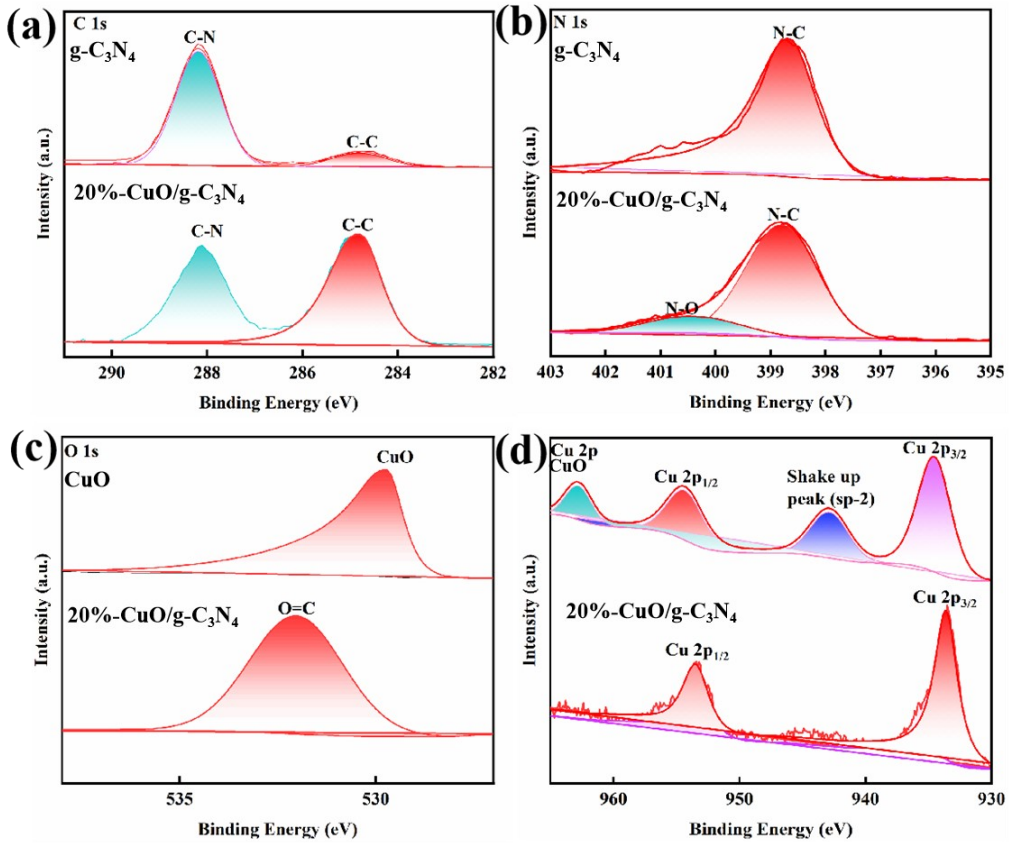

Fig. S5 The corresponding high-resolution XPS spectra of C 1s (a) N 1s (b), O 1s (c) and Cu 2p (d) of 20%-CuO/g-C_3N_4 in comparision with pure CuO and g-C_3N_4.

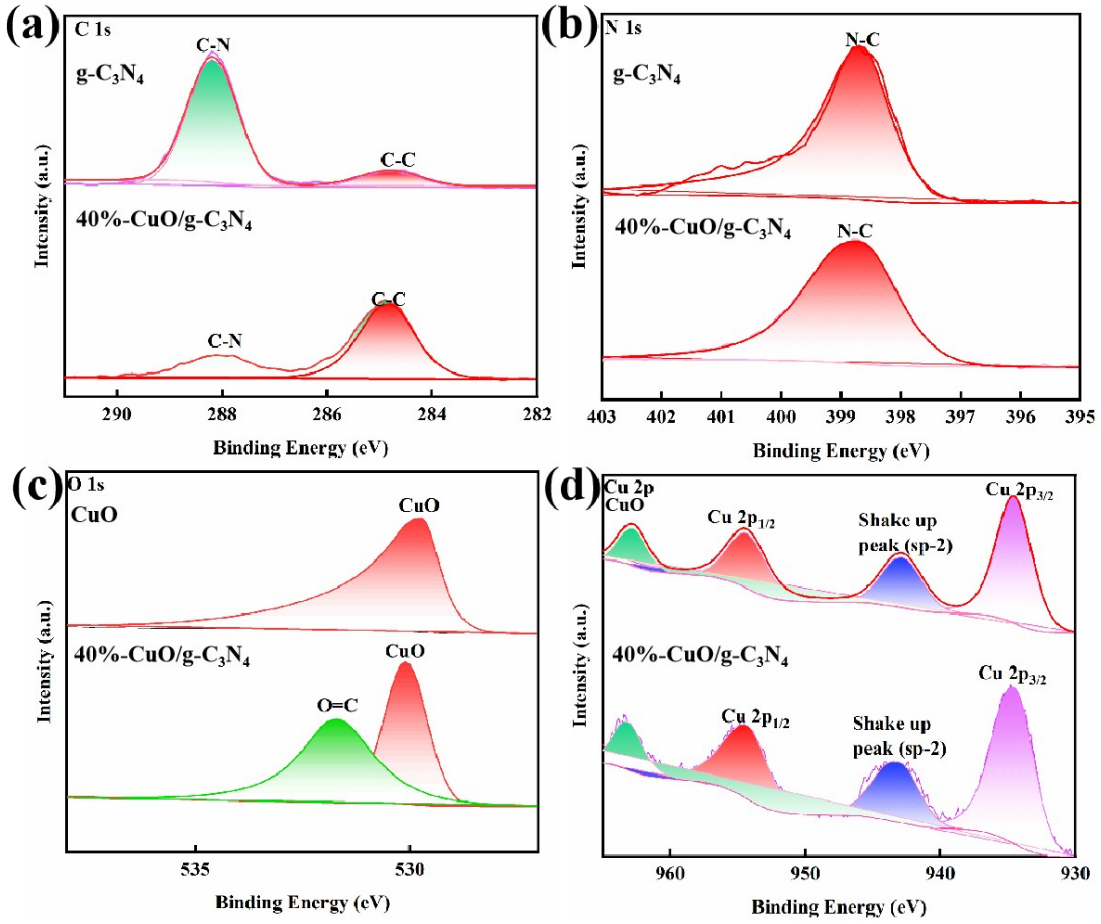

Fig. S6 The corresponding high-resolution XPS spectra of C 1s (a) N 1s (b), O 1s (c) and Cu 2p (d) of 40%-CuO/g-C_3N_4 in comparision with pure CuO and g-C_3N_4.

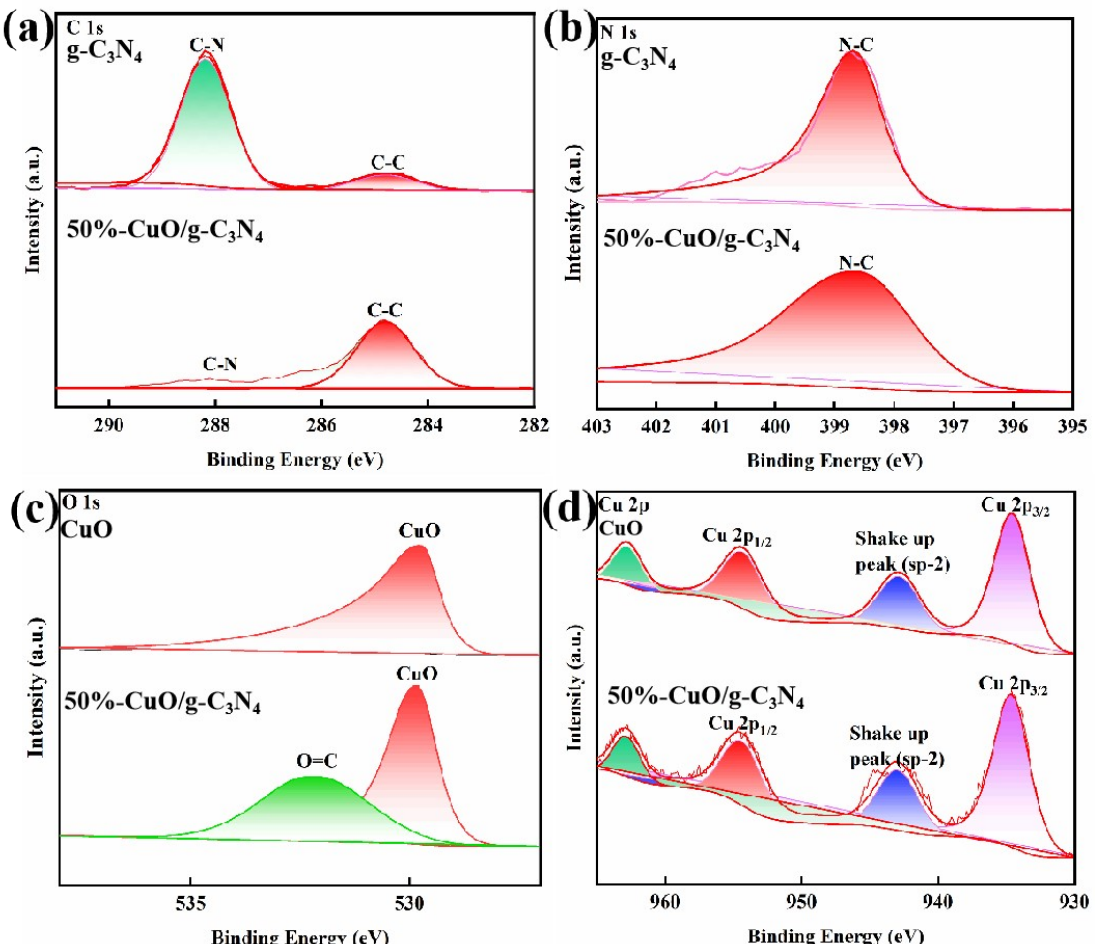

Fig. S7 The corresponding high-resolution XPS spectra of C 1s (a) N 1s (b), O 1s (c) and Cu 2p (d) of 50%-CuO/g-C_3N_4 in comparision with pure CuO and g-C_3N_4.

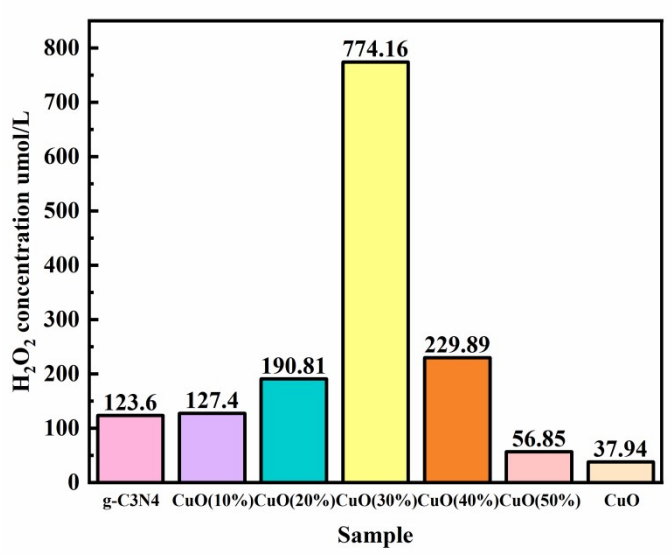

Fig. S8 Photocatalytic H_2O_2 production performance on CuO, g-C_3N_4 and CuO/g-C_3N_4 composite catalysts in pure water.

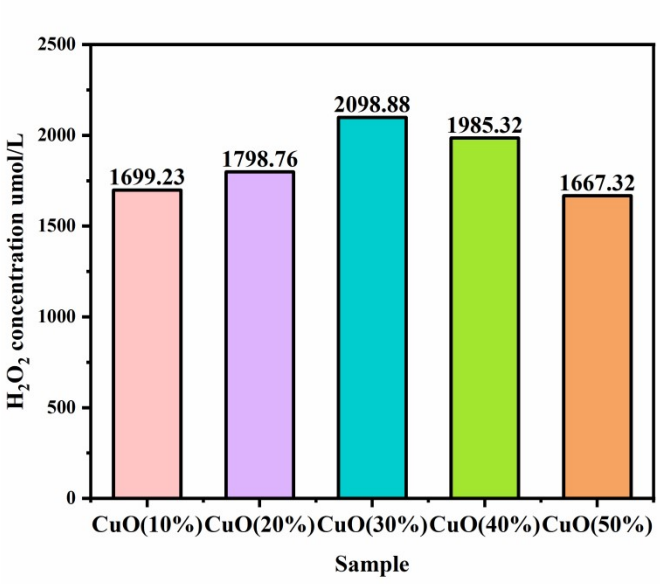

Fig. S9 Photocatalytic H_2O_2 production performance on CuO/g-C_3N_4 composite catalysts in water-HCl solution (v/v = 39:1).

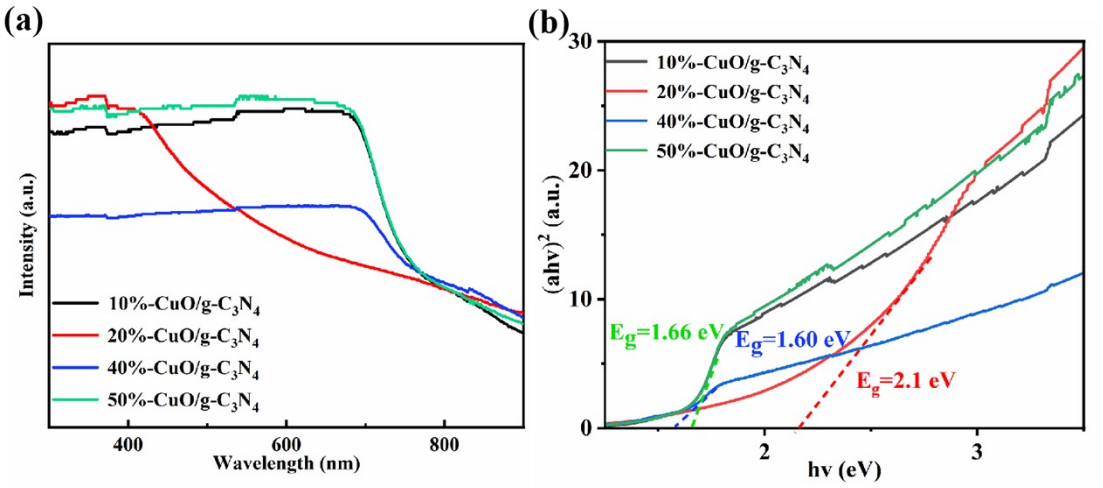

Fig. S10 UV-Vis spectra (a) and band gap of 10%-CuO/g-C_3N_4, 20%-CuO/g-C_3N_4, 40%-CuO/g-C_3N_4, 50%-CuO/g-C_3N_4

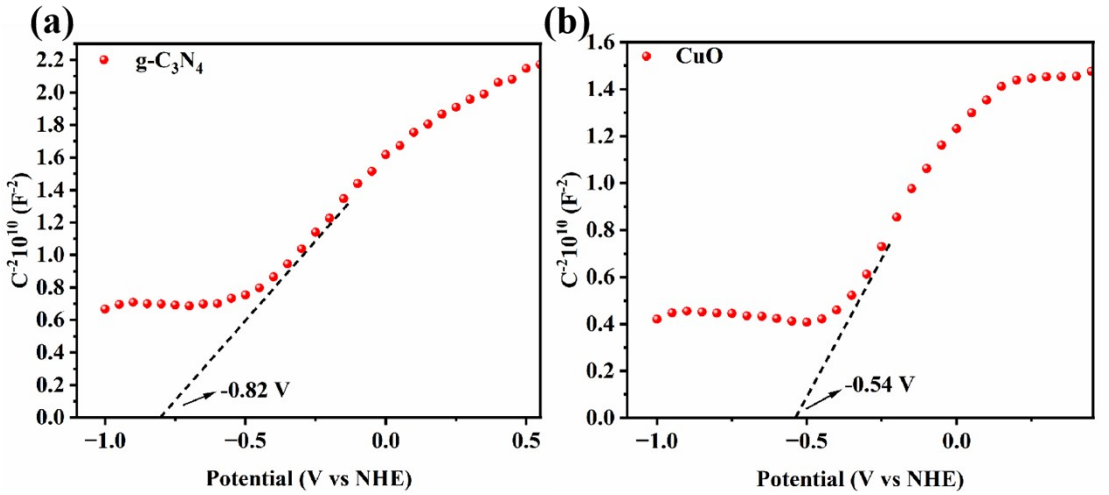

Fig. S11 Mott-Schottky of (a) g-C_3N_4 and (b) CuO.